Inorganica Chimica Acta 362 (2009) 4377–4388

Contents lists available at ScienceDirect

Inorganica Chimica Acta

journal homepage: www.elsevier.com/locate/ica

Metal complexes of new scorpionate ligands: 2,2′-Bis(pyrazolyl)ethylamine and its derivatives

Daniel L. Reger [a,*], Bryn Reinecke [a], Mark D. Smith [a], Radu F. Semeniuc [b]

[a] Department of Chemistry and Biochemistry, University of South Carolina, Columbia, SC 29208, USA
[b] Department of Chemistry, Eastern Illinois University, Charleston, IL 61920, USA

ARTICLE INFO

Article history:
Received 1 December 2008
Received in revised form 31 May 2009
Accepted 3 June 2009
Available online 9 June 2009

Dedicated to the memory of Swiatoslaw ("Jerry") Trofimenko.

Keywords:
Bis(pyrazolyl)amine ligands
Copper(I) triphenylphosphine
Scorpionate ligands
Non-covalent interactions

ABSTRACT

The new bis(pyrazolyl)amine ligand $NH_2CH_2CH(pz)_2$ (**1**) was prepared from the reaction of N-[2,2-bis(pyrazolyl)ethyl]-1,8-naphthalimide with hydrazine monohydrate. A substituted derivative, $C_6H_5CH_2NHCH_2CH(pz)_2$ (**2**), was prepared by the reaction of **1** with benzaldehyde followed by reduction with $NaBH_4$. Ligand **1** was also converted by two methods to the new bitopic, *para*-linked bis(pyrazolyl)amine ligand *p*-$C_6H_4(CH_2NHCH_2CH(pz)_2)_2$, (**3**). The reactions of the ligands **1**–**3** with $[Cu(PPh_3)_2]NO_3$ yields $\{(PPh_3)Cu[(pz)_2CHCH_2NH_2]\}NO_3$, $\{(PPh_3)Cu[(pz)_2CHCH_2NHCH_2C_6H_5]\}NO_3$ and $\{[(PPh_3)Cu]_2[p\text{-}((pz)_2CHCH_2NHCH_2)_2C_6H_4]\}(NO_3)_2\cdot$solvate, respectively. Complex $\{(N_3)_2Cu[(pz)_2CHCH_2NHCH_2C_6H_5]\}$ was obtained from a methanol solution of **2**, copper(II) acetate monohydrate and sodium azide. The complex $\{Cd[(pz)_2CHCH_2NHCH_2C_6H_5]_2\}(PF_6)_2\cdot 3C_3H_6O$ was synthesized by reaction of the protonated form of ligand **2**, $[(pz)_2CHCH_2NH_2CH_2C_6H_5]PF_6$, with $Cd(acac)_2$. In all of the structures the ligands are tridentate, bonding to the metal through the lone pair on the amine group as well as through the pyrazolyl rings – they act as true scorpionates. The solid state structures all have extensive non-covalent interactions, with the N–H functional groups of the amines participating in both N–H···π and N–H···O or N–H···N hydrogen bonding interactions.

© 2009 Elsevier B.V. All rights reserved.

1. Introduction

Supramolecular crystal engineering is an area of intense research because of its potential applications in materials design [1]. Important goals of this research are to understand how specific functional groups designed into the ligands of transition metal complexes will organize structure in a predictable fashion. Much of our research [2] in this area is derived from the poly(pyrazolyl)methane family of scorpionate ligands that was first introduced in 1970 by Trofimenko [3]. Building on his work, we reported "second generation" tris(pyrazolyl)methane ligands, ligands with bulky groups substituted at the 3-position of the pyrazolyl ring, another area first developed by Trofimenko with poly(pyrazolyl)borate ligands [4]. In order to control the organization of more complex supramolecular structures, we have prepared a series of "third generation" poly(pyrazolyl)methane ligands, ligands specifically functionalized at the non-coordinating "back" position as pictured in Chart 1 [2,5]. Metal complexes of these ligands have shown interesting molecular and supramolecular structures containing specific non-covalent interactions that can be controlled to some degree by altering the flexibility of the ligands, directional orientation of the poly(pyrazolyl)methane units and varying the poly(pyrazolyl)methane unit.

The ether linkage in ligands I–IX [2] was initially introduced for synthetic reasons and also to make these ligands semi-rigid so that metal complexes would have solubility in organic solvents and be more versatile for the self-assembly process. In addition, the lone pairs on the ether linkage frequently enter into weak hydrogen bonding interactions (C–H···O), interactions not possible with ligands X–XIV [5b,c]. Interestingly, in no case have we observed direct coordination of the ether oxygen to a metal.

In order to further manipulate and enhance the coordination possibilities for these types of poly(pyrazolyl)methane ligands, we have prepared ligands that incorporate amine functionalities into the bis(pyrazolyl)methane backbone. We anticipated that the amine N–H group would be capable of participating in supramolecular organization through strong hydrogen bonding interactions, augmenting the organizational features already observed by the ligands in Chart 1. Described here are the syntheses of the parent bis(pyrazolyl)amine $H_2NCH_2CH(pz)_2$ (pz=pyrazolyl), the benzyl-substituted bis(pyrazolyl)amine $C_6H_5CH_2NHCH_2CH(pz)_2$, and the bitopic, *para*-arene linked bis(pyrazolyl)amine *p*-$C_6H_4(CH_2NHCH_2CH(pz)_2)_2$ and the use of these new ligands for the syntheses and structural determinations of five metal complexes. While in certain cases the hydrogen(s) of the amine functionality is involved in hydrogen bonding, in all of the complexes the lone pair on the

---

* Corresponding author.
E-mail address: reger@mail.chem.sc.edu (D.L. Reger).

0020-1693/$ - see front matter © 2009 Elsevier B.V. All rights reserved.
doi:10.1016/j.ica.2009.06.004

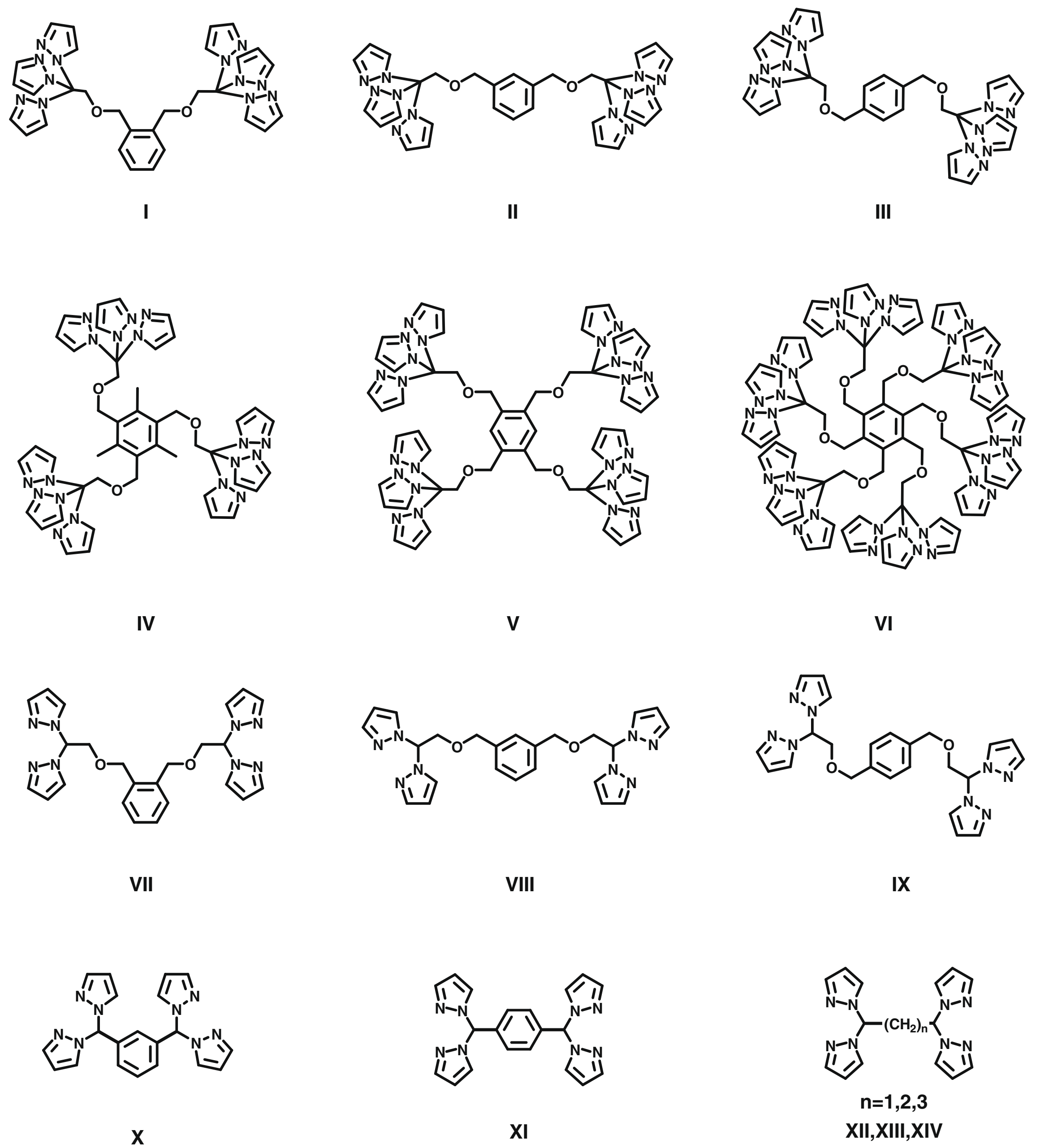

Chart 1. Third Generation Poly(pyrazolyl)methane Ligands.

amine nitrogen coordinates directly to the metal center, or as put in the terminology introduced by Trofimenko the scorpionate "stinger" is striking its prey. Some of these results have previously been communicated [6].

2. Results

2.1. Synthesis

N-[2,2-bis(pyrazolyl)ethyl]-1,8-naphthalimide [2a], prepared earlier by us, was found to react with hydrazine monohydrate to release the parent bis(pyrazolyl)amine, $NH_2CH_2CH(pz)_2$, (**1**) (Scheme 1). The benzyl derivative of this compound was made by reaction of **1** with benzaldehyde followed by reduction with $NaBH_4$ to give $C_6H_5CH_2NHCH_2CH(pz)_2$, (**2**). The parent amine **1** also reacts with half an equivalent of dibromo-*para*-xylene in THF in the presence of triethylamine to give the new para-linked bis(pyrazolyl)amine product *p*-$C_6H_4(CH_2NHCH_2CH(pz)_2)_2$ (**3**, Scheme 2). The initial product isolated from this method was impure, so it was further recrystallized from ethanol to yield a beige powder, but this process lowered the yield significantly. Subsequently, it was discovered that the condensation of **1** with terephthaldehyde followed by reduction with sodium borohydride in methanol gave **3** in much higher yield.

The complexes $\{(PPh_3)Cu[(pz)_2CHCH_2NH_2]\}NO_3$ (**4**), $\{(PPh_3)Cu[(pz)_2CHCH_2NHCH_2C_6H_5]\}NO_3$ (**5**) and $\{[(PPh_3)Cu]_2[p\text{-}((pz)_2CHCH_2NHCH_2)_2C_6H_4]\}(NO_3)_2$·solvate (**8**), were prepared by the reaction of the ligands **1**, **2** and **3**, respectively, and an appropriate ratio of $[Cu(PPh_3)_2]NO_3$ in dichloromethane, followed by addition of hexanes to precipitate the products. Crystals of $\{(N_3)_2Cu[(pz)_2CHCH_2NHCH_2C_6H_5]\}$ (**6**) were obtained by dissolving **2** in dichloromethane and layering with a solution of copper(II) acetate

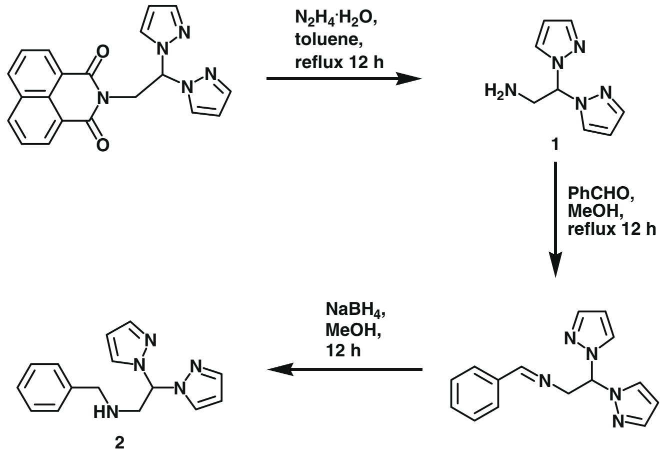

Scheme 1. Synthesis of ligands **1** and **2**.

monohydrate and sodium azide in methanol. Crystals of $\{Cd[(pz)_2CHCH_2NHCH_2C_6H_5]_2\}(PF_6)_2{\cdot}3C_3H_6O$ (**7**) were obtained by reaction of the protonated form of ligand **2**, $[(pz)_2CHCH_2NH_2CH_2C_6H_5]PF_6$, with $Cd(acac)_2$ followed by crystallization from acetone/diethyl ether.

2.2. Solid state structure analysis

Crystallographic data are listed in Tables 1 and 2. Selected bond lengths and angles are shown in Tables 3–5. Hydrogen bonding parameters are listed in Table 6. The most important result evident in all of the structures is that the ligands are tridentate, bonding to the metal through the lone pair on the amine group as well as through the pyrazolyl rings. There is substantial supramolecular organization in all of the structures.

In the crystal structure containing the parent bis(pyrazolyl)amine, $\{(PPh_3)Cu[(pz)_2CHCH_2NH_2]\}NO_3$ (**4**, Fig. 1), the copper is in a pseudotetrahedral environment coordinated to the amine nitrogen, two pyrazolyl nitrogens, and a triphenyphosphine group. The main distortion is caused by the restricted “bite” of the 6-membered chelate rings of the ligand **1** that lowers the N–Cu–N angles to approximately 90°. The one dimensional supramolecular structure is organized by concerted N–H$\cdots\pi$ and C–H$\cdots\pi$ interactions to form cationic chains (Fig. 2). The N–H$\cdots\pi$ interactions occur between one of the NH_2 hydrogens oriented toward one of the phenyl rings in the triphenylphosphine moiety on a neighboring cation. The H$\cdots$centroid and N$\cdots$centroid distances are 2.59 Å and 3.50 Å, respectively. The nearly linear N–H$\cdots$centroid angle of 171° shows that the hydrogen atom is almost centered over the phenyl ring. The phenyl ring that serves as the proton acceptor in the N–H$\cdots\pi$ interaction previously described becomes the hydrogen donor in the C–H$\cdots\pi$ interaction. A hydrogen atom from this ring is directed toward another triphenylphosphine phenyl ring from the first molecule in the previous interaction. The H$\cdots$centroid and C$\cdots$centroid distances are 2.69 Å and 3.47 Å, respectively, with a C–H$\cdots$centroid angle of 140°, again showing that the hydrogen is almost centered over the phenyl ring with which it interacts. These chains are linked together into a cationic sheet by hydrogen bonding of CH and NH groups through bridging nitrate counterions (Fig. 3). The NH_2 hydrogen that is not used in the N–H$\cdots\pi$ interaction forms a hydrogen bond to a nitrate oxygen with H$\cdots$O and N$\cdots$O bond distances of 2.18 Å and 3.08 Å and an N–H$\cdots$O angle of 165°. The $CH(pz)_2$ hydrogen from a different chain forms a hydrogen bond to a second oxygen atom on the same nitrate anion with C$\cdots$H and C$\cdots$O distances of 2.38 Å and 3.29 Å, respectively and a C–H$\cdots$O angle of 151°. The overall structure is a two dimensional sheet.

The analogous complex of the benzyl ligand **2**, $\{(PPh_3)Cu[(pz)_2CHCH_2NHCH_2C_6H_5]\}NO_3$ (**5**), also has the copper in a pseudotetrahedral environment with tridentate coordination of the ligand and the fourth position occupied by triphenylphosphine (Fig. 4). Likely due to the increased steric hindrance introduced by the benzyl group, no N–H$\cdots\pi$ interactions are present in the cationic chains. Nevertheless, the cations are still arranged in chains by C–H$\cdots\pi$ interactions identical to those in **4**. A hydrogen atom from a triphenylphosphine phenyl group interacts with a phenyl group from a neighboring triphenylphosphine (Fig. 5). The H$\cdots$centroid and C$\cdots$centroid distances are 2.97 Å and 3.86 Å, respectively, with a

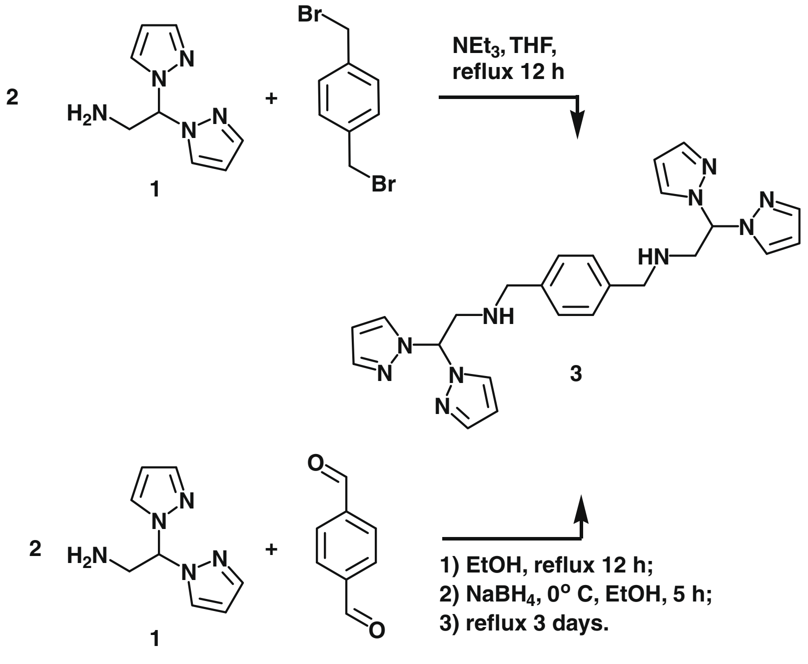

Scheme 2. Syntheses of ligand **3**.

Table 1
Crystallographic information for $\{(PPh_3)Cu[(pz)_2CHCH_2NH_2]\}NO_3$ (**4**) and $\{(PPh_3)Cu[(pz)_2CHCH_2NHCH_2C_6H_5]\}NO_3 \cdot 1.5C_2H_2Cl_2$ (**5**$\cdot 1.5CH_2Cl_2$).

	4	(**5**$\cdot 1.5CH_2Cl_2$)
Empirical formula	$C_{26}H_{26}CuN_6O_3P$	$C_{34.50}H_{35}Cl_3CuN_6O_3P$
Formula weight	565.04	782.54
Temperature	150(1) K	150(1) K
Wavelength	0.71073 Å	0.71073 Å
Crystal system	monoclinic	triclinic
Space group	$P2_1/c$	$P\bar{1}$
Unit cell dimensions	a = 14.4251(7) Å b = 14.9688(8) Å c = 13.4458(7) Å	a = 8.3448(5) Å b = 11.0671(6) Å c = 19.4718(11) Å
Unit cell angles	α = 90° β = 116.130(1)° γ = 90°	α = 83.351(1)° β = 86.171(1)° γ = 83.428(1)°
Volume	2606.6(2) $Å^3$	1771.83(17) $Å^3$
Z	4	2
Density (calculated)	1.440 Mg/m^3	1.467 Mg/m^3
Absorption coefficient	0.939 mm^{-1}	0.932 mm^{-1}
F (0 0 0)	1168	806
Crystal size	0.48 × 0.10 × 0.08 mm^3	0.52 × 0.30 × 0.18 mm^3
Reflections collected	21088	19189
Independent reflections	4613 [R(int) = 0.0692]	7256 [R(int) = 0.0241]
Absorption correction	none	Semi-empirical from equivalents
Refinement method	full-matrix least-squares on F^2	full-matrix least-squares on F^2
Goodness-of-fit (GoF) on F^2	0.960	1.041
Final R indices [$I > 2\sigma(I)$]	R_1 = 0.0436, wR_2 = 0.0868	R_1 = 0.0371, wR_2 = 0.0987
R indices (all data)	R_1 = 0.0597, wR_2 = 0.0921	R_1 = 0.0397, wR_2 = 0.1007

Table 2
Crystallographic information for $\{(N_3)_2Cu[(pz)_2CHCH_2NHCH_2C_6H_5]\}$ (**6**), $\{Cd[(pz)_2CHCH_2NHCH_2C_6H_5]_2\}(PF_6)_2 \cdot 3C_3H_6O$ (**7**), and $\{[(PPh_3)Cu]_2[p\text{-}((pz)_2CHCH_2NHCH_2)_2\text{-}C_6H_4]\}(NO_3)_2 \cdot$solvate (**8**).

	6	**7**	**8**
Empirical formula	$C_{15}H_{17}CuN_{11}$	$C_{39}H_{52}CdF_{12}N_{10}O_3P_2$	$C_{60}H_{58}Cu_2N_{12}O_6P_2$
Formula weight	414.94	1111.25	1232.20
Temperature	150(1) K	150(1) K	150(1) K
Wavelength	0.71073 Å	0.71073 Å	0.71073 Å
Crystal system	triclinic	triclinic	triclinic
Space group	$P\bar{1}$	$P\bar{1}$	$P\bar{1}$
Unit cell dimensions	a = 7.6788(3) Å b = 13.3868(6) Å c = 19.2509(8) Å	a = 10.8757(7) Å b = 11.1856(7) Å c = 12.1212(8) Å	a = 10.1775(9) Å b = 11.9295(10) Å c = 15.5942(13) Å
Unit cell angles	α = 71.920(1)° β = 86.317(1)° γ = 73.553(1)°	α = 91.616(1)° β = 113.326(1)° γ = 114.490(1)°	α = 110.561(2)° β = 92.662(2)° γ = 93.415(2)°
Volume	1803.60(13) $Å^3$	1199.14(13) $Å^3$	1765.0(3) $Å^3$
Z	4	1	1
Density (calculated)	1.528 Mg/m^3	1.539 Mg/m^3	1.159 Mg/m^3
Absorption coefficient	1.237 mm^{-1}	0.616 mm^{-1}	0.699 mm^{-1}
F (0 0 0)	852	566	638
Crystal size	0.40 × 0.18 × 0.04 mm^3	0.42 × 0.32 × 0.24 mm^3	0.30 × 0.20 × 0.14 mm^3
Reflections collected	18369	13579	11707
Independent reflections	6358 [R(int) = 0.0634]	4908 [R(int) = 0.0351]	4078 [R(int) = 0.0468]
Refinement method	full-matrix least-squares on F^2	full-matrix least-squares on F^2	full-matrix least-squares on F^2
Goodness-of-fit (GoF) on F^2	0.968	1.037	0.981
Final R indices [$I > 2\sigma(I)$]	R_1 = 0.0354, wR_2 = 0.0797	R_1 = 0.0255, wR_2 = 0.0657	R_1 = 0.0444, wR_2 = 0.1118
R indices (all data)	R_1 = 0.0440, wR_2 = 0.0826	R_1 = 0.0261, wR_2 = 0.0660	R_1 = 0.0518, wR_2 = 0.1144

C–H⋯centroid angle of 159°, again showing that the hydrogen atom is almost centered over the phenyl ring. The nitrate counterions link the chains together into sheets with N–H⋯O and C–H⋯O hydrogen bonds in the same manner as compound **4**. One hydrogen bond is made by the N–H and has H⋯O and N⋯O distances of 2.21 Å and 2.97 Å with a N–H⋯O angle of 157°. The other hydrogen bond is through a methine hydrogen from $CH(pz)_2$ to the same nitrate anion with H⋯O and C⋯O distances of 2.36 Å and 3.31 Å and a C–H⋯O angle of 156°. The benzyl functionality results in additional interactions that organize compound **5** into a three dimensional structure. The *para*-hydrogen from the benzyl group interacts with a pyrazolyl ring in a C–H⋯π interaction with H⋯centroid and C⋯centroid distances of 2.99 Å and 3.73 Å, respectively and a C–H⋯centroid angle of 137° (Fig. 6).

In the copper azide complex $\{(N_3)_2Cu[(pz)_2CHCH_2NHCH_2C_6H_5]\}$ (**6**), the copper is in a pseudo-square pyramidal environment with three coordination sites occupied by ligand **2** in the usual tridentate arrangement with the remaining two bonds being to the azide groups (Fig. 7). One of the pyrazolyl ring donor atoms, N21, occupies the axial site. Supramolecular interactions include two concerted N–H⋯N hydrogen bonds between the amine hydrogen on one molecule to an azide nitrogen bonded to the copper atom on a neighboring molecule of the complex and a reciprocal N–H⋯N bond from the amine hydrogen on the second molecule to an azide

Table 3
Selected bond lengths (Å) and angles (°) for **4** and **5**·1.5CH$_2$Cl$_2$.

4		**5**·1.5CH$_2$Cl$_2$	
Cu(1)–N(21)	2.053(3)	Cu(1)–N(11)	2.0645(17)
Cu(1)–N(11)	2.116(2)	Cu(1)–N(21)	2.0700(17)
Cu(1)–N(1)	2.145(2)	Cu(1)–N(1)	2.1296(17)
Cu(1)–P(1)	2.1631(9)	Cu(1)–P(1)	2.1542(5)
N(21)–Cu(1)–N(11)	89.26(10)	N(11)–Cu(1)–N(21)	90.06(7)
N(21)–Cu(1)–N(1)	89.72(10)	N(11)–Cu(1)–N(1)	89.12(7)
N(11)–Cu(1)–N(1)	85.95(9)	N(21)–Cu(1)–N(1)	88.75(7)
N(21)–Cu(1)–P(1)	132.33(7)	N(11)–Cu(1)–P(1)	132.97(5)
N(11)–Cu(1)–P(1)	124.11(7)	N(21)–Cu(1)–P(1)	121.37(5)
N(1)–Cu(1)–P(1)	122.18(7)	N(1)–Cu(1)–P(1)	122.34(5)

Table 4
Selected bond lengths (Å) and angles (°) for **6** and **7**.

6		**7**	
Cu(1)–N(54)	1.969(2)	Cd(1)–N(11)	2.3039(14)
Cu(1)–N(51)	1.985(2)	Cd(1)–N(21)	2.3424(13)
Cu(1)–N(11)	2.021(2)	Cd(1)–N(1A[a])	2.377(2)
Cu(1)–N(1)	2.059(2)	N(11)–Cd(1)–N(11a)	180
Cu(1)–N(21)	2.250(2)	N(11)–Cd(1)–N(21)	81.77(5)
Cu(2)–N(64)	1.967(2)	N(11)–Cd(1)–N(1A)	86.43(7)
Cu(2)–N(61)	2.000(2)	N(21)–Cd(1)–N(1A)	74.24(7)
Cu(2)–N(31)	2.030(2)	N(11)–Cd(1)–N(21a)	98.23(5)
Cu(2)–N(2)	2.058(2)	N(11)–Cd(1)–N(1Aa)	93.57(7)
Cu(2)–N(41)	2.249(2)	N(21)–Cd(1)–N(1Aa)	105.76(7)
N(54)–Cu(1)–N(51)	93.58(9)		
N(54)–Cu(1)–N(11)	92.92(8)		
N(51)–Cu(1)–N(11)	170.53(8)		
N(54)–Cu(1)–N(1)	164.83(9)		
N(51)–Cu(1)–N(1)	87.58(9)		
N(11)–Cu(1)–N(1)	84.36(8)		
N(54)–Cu(1)–N(21)	104.33(8)		
N(51)–Cu(1)–N(21)	99.23(8)		
N(11)–Cu(1)–N(21)	85.81(8)		
N(1)–Cu(1)–N(21)	90.38(8)		
N(64)–Cu(2)–N(61)	93.44(9)		
N(64)–Cu(2)–N(31)	93.84(9)		
N(61)–Cu(2)–N(31)	168.66(9)		
N(64)–Cu(2)–N(2)	167.36(9)		
N(61)–Cu(2)–N(2)	86.91(9)		
N(31)–Cu(2)–N(2)	84.09(8)		
N(64)–Cu(2)–N(41)	102.42(9)		
N(61)–Cu(2)–N(41)	100.43(8)		
N(31)–Cu(2)–N(41)	86.47(8)		
N(2)–Cu(2)–N(41)	89.93(8)		

[a] A = dominant disorder orientation.

Table 5
Selected bond lengths (Å) and angles (°) for **8**.

Cu(1)–N(21)	2.041(3)
Cu(1)–N(11)	2.068(3)
Cu(1)–P(1)	2.1450(11)
Cu(1)–N(1)	2.155(3)
N(21)–Cu(1)–N(11)	90.93(12)
N(21)–Cu(1)–P(1)	130.82(9)
N(11)–Cu(1)–P(1)	124.93(10)
N(21)–Cu(1)–N(1)	88.79(11)
N(11)–Cu(1)–N(1)	87.63(12)
P(1)–Cu(1)–N(1)	121.31(8)

Table 6
Hydrogen bonding parameters for **4**–**8**, lengths (Å) and angles (°).

Atoms	D···A	H···A	D–H···A
4			
N(1)–H(1B)···O(1)	3.077(3)	2.18	165
C(1)–H(1)···O(3)	3.297(4)	2.38	151
***5**·1.5CH$_2$Cl$_2$*			
N(1)–H(1A)···O(1)	2.974(2)	2.21(3)	157(2)
C(1)–H(1)···O(3)	3.301(3)	2.36	156
6			
N(1)–H(1N)···N(51)#1	3.094(3)	2.348(18)	150(2)
N(2)–H(H2N)···N(61)#2	3.156(3)	2.430(16)	149(2)
7			
N(1A)–H(1NA)···O(1)	3.344(3)	2.51(3)	178(3)
8			
N(1)–H(1N)···O(1)	2.958(5)	2.10(4)	147(3)
C(1)–H(1)···O(1)#2	3.250(5)	2.32	155
C(1)–H(1)···O(2)#2	3.446(5)	2.52	154

Symmetry codes: **6**, #1 = 1 − *x*, 1 − *y*, *z*, #2 = 1 − *x*, 1 − *y*, 1 − *z*; **8**, #2 = −*x*, 1 − *y*, 1 − *z*.

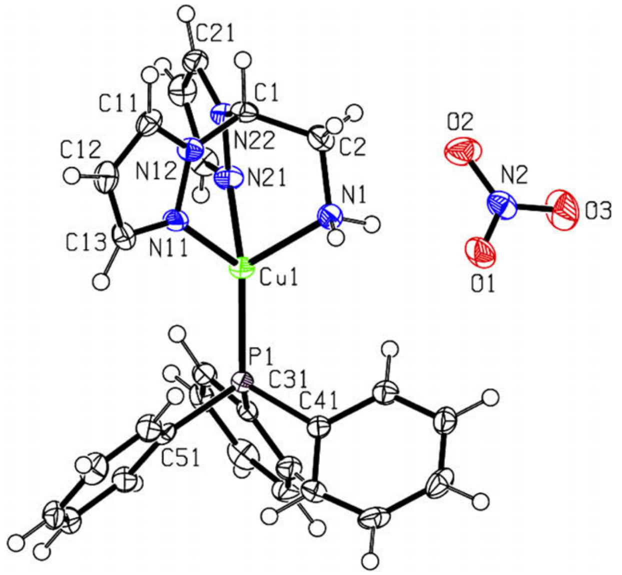

Fig. 1. ORTEP diagram of {(PPh$_3$)Cu[(pz)$_2$CHCH$_2$NH$_2$]}NO$_3$ (**4**).

nitrogen on the first (Fig. 8). The N···H and N···N lengths are 2.35 Å and 3.09 Å, respectively, and the N–H···N angle is 150° for one bond. The lengths for the second bond are similar at 2.43 Å and 3.16 Å with an N–H···N angle of 149°. Two pyrazolyl rings on neighboring "dimers" formed by the two N–H···N hydrogen bonds participate in a π–π stack with a centroid···centroid distance of 3.527 Å and a slip angle of 13°. These stacked rings each have a C–H bond pointed directly toward a pyrazolyl ring oriented perpendicularly to the stack which results in a C–H···π interaction. The H···centroid distances are 2.73 Å and 2.74 Å and the C···centroid distances are 3.52 Å and 3.36 Å with C–H···centroid angles of 142° and 144°. This interaction containing one π–π stack and two C–H···π interactions is known as the pyrazolyl embrace [2e], and it serves to link the hydrogen-bound asymmetric units into chains. Other C–H···N hydrogen bonds occur between hydrogens on the pyrazolyl rings and terminal azide nitrogens on neighboring chains to give 2D sheets with C···N and N···H lengths of 3.44 Å and 2.53 Å, respectively with a C–H···N angle of 161° (Fig. 9). These sheets are then linked into a 3D structure by C–H···N hydrogen bonds between the CH(pz)$_2$ methine hydrogen and an azide nitrogen. The C···N and N···H distances are 3.31 Å and 2.35 Å, respectively with a C–H···N angle of 160°.

Two tridentate ligands of **2** bond to cadmium(II) in {Cd[(pz)$_2$CHCH$_2$NHCH$_2$C$_6$H$_5$]$_2$}(PF$_6$)$_2$·3C$_3$H$_6$O (**7**) to yield a pseudo-octahedral environment around the metal (Fig. 10). There is disorder in the benzyl region of the molecule over two closely spaced orientations in the refined ratio *A*/*B* = 0.701(4)/0.299(4). Only the

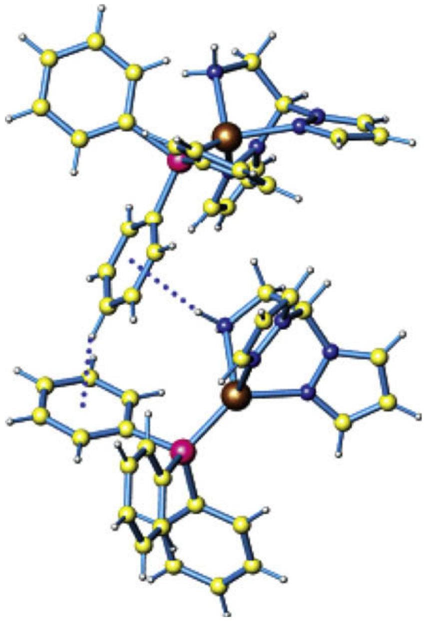

Fig. 2. Self-assembly of {(PPh$_3$)Cu[(pz)$_2$CHCH$_2$NH$_2$]}$^+$ in **4** into chains through N–H···π and C–H···π interactions.

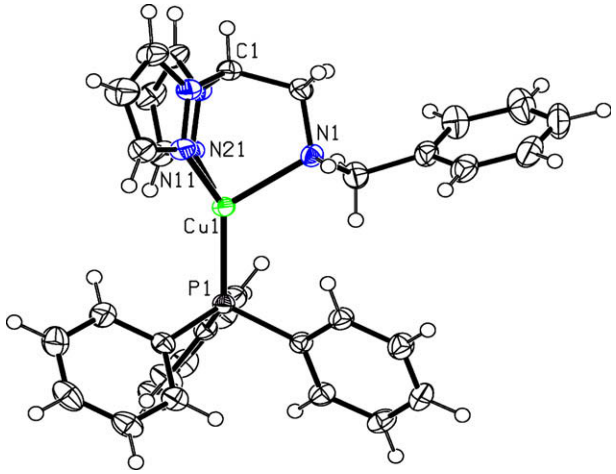

Fig. 4. ORTEP diagram of the {(PPh$_3$)Cu[(pz)$_2$CHCH$_2$NHCH$_2$C$_6$H$_5$]}$^+$ building block of **5**·1.5CH$_2$Cl$_2$. Displacement ellipsoids drawn at the 50% probability level.

A orientation is examined here. In the crystal, the only supramolecular interaction observed is a C–H···π interaction between a hydrogen from the backbone carbon nearest the benzyl ring to a benzyl ring from a neighboring molecule of the complex (Fig. 11). The H···centroid and C···centroid distances are 2.99 Å and 3.88 Å, respectively, with a C–H···centroid angle of 150°. Although this appears to be a strong interaction, there is a great deal of disorder in this region of the structure so the non-covalent interactions cannot be analyzed definitively.

The bitopic bridging ligand **3**, analogous to the ether linked ligand IX in Chart 1, was prepared in order to build a more highly organized covalent architecture. Fig. 12 shows the structure of its dinuclear copper(I) triphenylphosphine adduct, {[(PPh$_3$)Cu]$_2$[*p*-((pz)$_2$CHCH$_2$NHCH$_2$)$_2$C$_6$H$_4$]}(NO$_3$)$_2$·solvate (**8**). Each end of the *para*-linked bis(pyrazolyl)amine ligand coordinates in the same tridentate manner as bis(pyrazolyl)amine ligands **1** and **2**. The supramolecular interactions include one hydrogen bond between the amine hydrogen and the nitrate counterion, as well as a bifurcated bond from the CH(pz)$_2$ methine hydrogen to two oxygen atoms on the same nitrate anion, thus linking the individual bimetallic units into one dimensional ribbons (Fig. 13). The N–H···O hydrogen bonds form with H···O and N···O lengths of 2.10 Å and 2.96 Å, respectively and an N–H···O angle of 147°. The bifurcated C–H···O bonds form from the CH(pz)$_2$ methine hydrogen to the nitrate anion with H···O and C···O bond lengths of 2.33 Å and 2.52 Å, and 3.25 Å and 3.45 Å, respectively, with C–H···O angles of 154° and 155°. These ribbons are further linked into two dimensional sheets by π–π stacks between two phenyl rings on neighboring units with a centroid-centroid distance of 4.09 Å and slip angle of 25° (Fig. 14).

3. Discussion

The most important result of this investigation is that the new amine substituted bis(pyrazolyl)methane ligands coordinate to the metal atom in a tridentate manner with fairly similar M–N bond distances in all five complexes studied – they act as true scorpionates. This result was unexpected because in the ether analogues, the ligands only coordinated in a bidentate fashion through the pyrazolyl ring donor atoms; the oxygen atoms of the ether link only participate in the non-covalent structure.

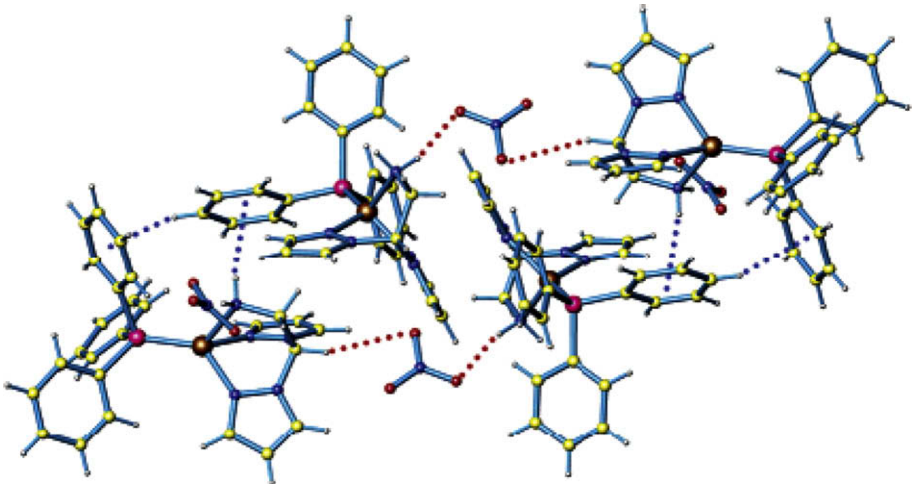

Fig. 3. 2D organization of **4** via D–H···π interactions (D= C, N); (blue dotted lines) and D–H···O hydrogen bonds (red dotted lines). (For interpretation of the references to colour in this figure legend, the reader is referred to the web version of this article.)

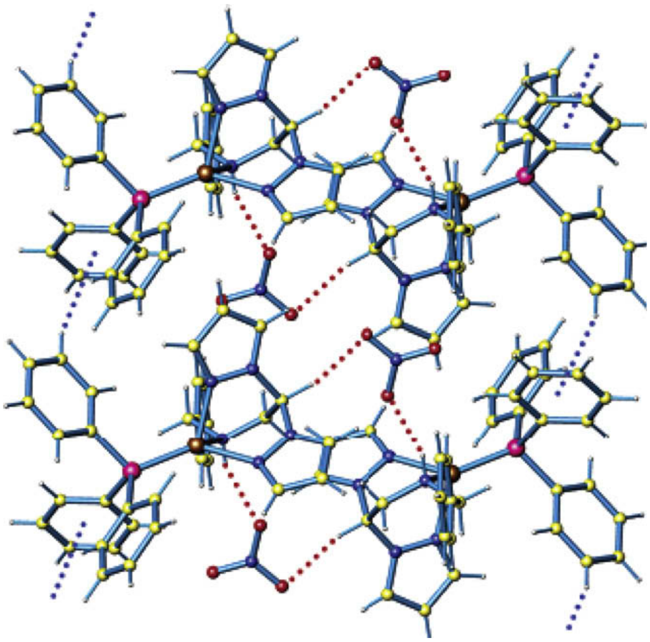

Fig. 5. 2D supramolecular organization of **5**·1.5CH_2Cl_2 via C–H···π interactions (dotted blue lines) and N–H···O and C–H···O hydrogen bonds (dotted red lines). (For interpretation of the references to colour in this figure legend, the reader is referred to the web version of this article.)

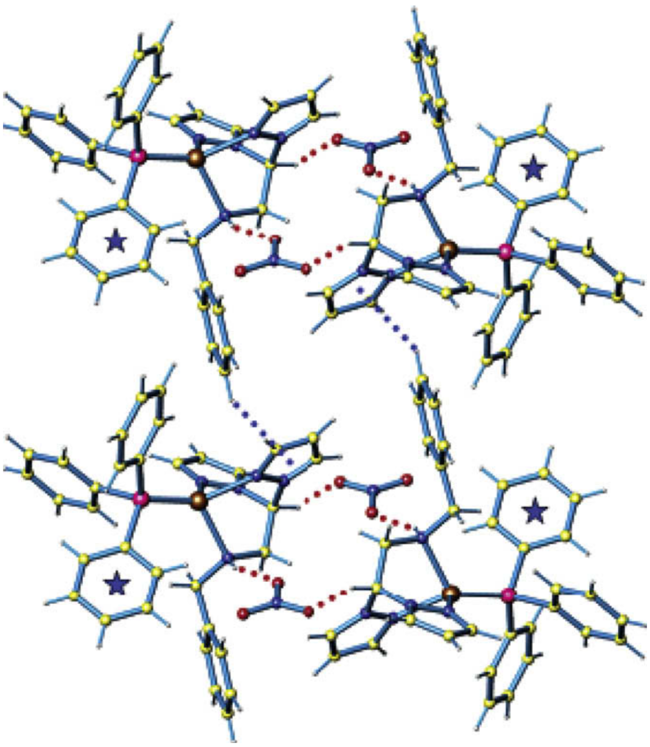

Fig. 6. 3D architecture of **5**·1.5CH_2Cl_2, based on a C–H···π interaction between the benzyl group and a pyrazolyl ring. The phenyls marked with a star are those that act as hydrogen receptors in the chain formation shown in Fig. 5.

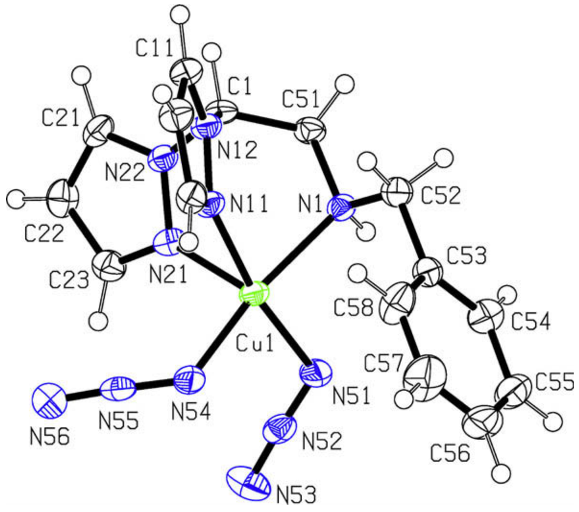

Fig. 7. ORTEP diagram of one molecule of $\{(N_3)_2Cu[(pz)_2CHCH_2NHCH_2C_6H_5]\}$ (**6**).

The goal of using the N–H functional groups of the amines to build extensive non-covalent interactions was successful. In the three structures with nitrate counterions, **4**, **5** and **8**, N–H···O hydrogen bonding with this ion is an important organizational feature. Interestingly, N–H···π interactions also are very important. For example, in the sheet structure of **4** the NH_2 group forms both a N–H···π and N–H···O hydrogen bonding interaction. The structure of **5** is similar, but the addition of the benzyl group blocks the N–H···π interaction, with this new functionality adding additional organizing features that lead to a three dimensional supramolecular structure. In addition to these non-covalent interactions, the bimetallic structure of **8** is also organized by the bitopic linking arrangement of the two bis(pyrazolyl)amine units in each ligand.

In the neutral, diazide structure of **6** hydrogen bonding from the ligand is still an important non-covalent force, with the nitrogens of the azide ligands coordinated to the copper(II) acting as the donor group in the hydrogen bonding. In addition to this interaction, we observe the cooperative π–π stack/two C–H···π interactions known as the pyrazolyl embrace, a feature that we have characterized previously as an important non-covalent interaction present in the structures of many metal complexes of poly(pyrazolyl)methane and poly(pyrazolyl)borate ligands [2e]. Compound **7** is a typical six-coordinate complex of Cd(II).

4. Experimental

4.1. General considerations

Starting materials were purchased from Aldrich. ^1H NMR spectra were recorded on a Varian AM300 spectrometer using a broadband probe. Proton chemical shifts are reported in ppm versus internal $(CH_3)_4Si$. Mass spectral data were recorded on either a MicroMass QTOF spectrometer or a VG70S instrument. Elemental analyses were performed by Robinson Microlit, Madison, NJ. N-[2,2-bis(pyrazolyl)ethyl]-1,8-naphthalimide was prepared as reported previously [2a].

4.2. Synthesis of $H_2NCH_2CH(pz)_2$ (*1*)

N-[2,2-bis(pyrazolyl)ethyl]-1,8-naphthalimide (40.00 g, 0.11 mol) was dissolved completely in warm toluene (250 mL). Hydrazine monohydrate (40 mL, 98%, 0.83 mol) was added and the mixture was heated at reflux overnight. After cooling to room temperature, the toluene and excess hydrazine were removed by rotary evaporation and the product, 2,2-dipyrazol-1-yl-ethylamine, **1**, dried under vacuum. The solid was dissolved in two 100 mL portions of H_2O and these solutions filtered. The water was removed via rotary evaporation to yield the product as an oily

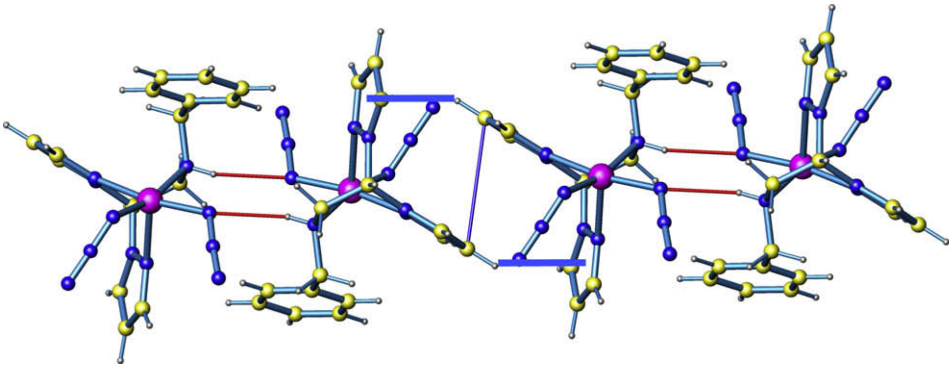

Fig. 8. N–H· · ·N hydrogen bonding (red lines) between two molecules of **6** creates centrosymmetric dimers, π–π and C–H· · ·π interactions between dimers (blue lines) organizes them into chains. (For interpretation of the references to colour in this figure legend, the reader is referred to the web version of this article.)

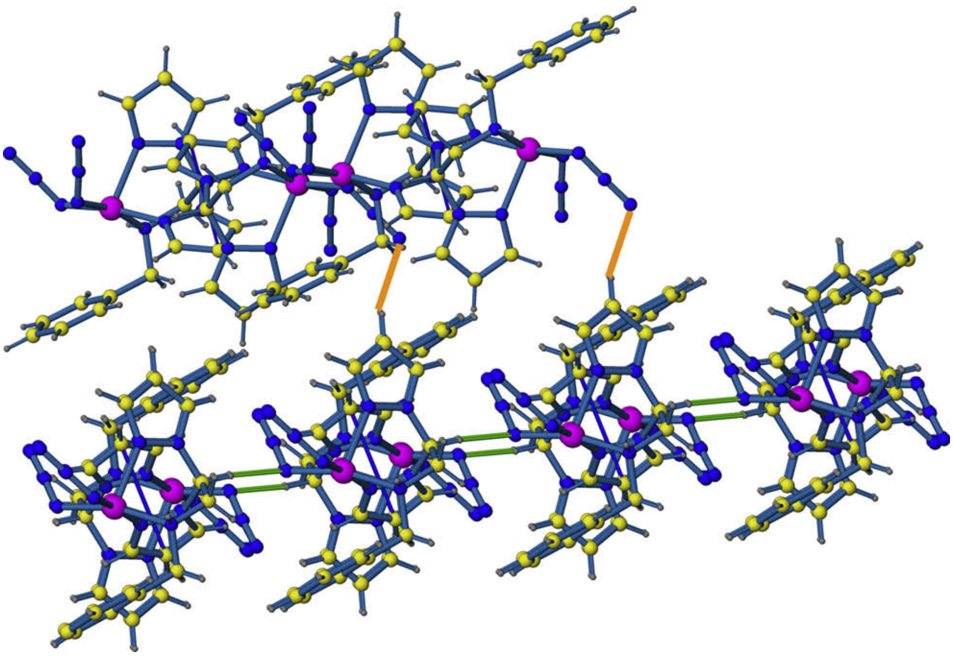

Fig. 9. C–H· · ·N hydrogen bonding in the plane perpendicular to the plane in Fig. 8 (orange and green lines) organizes chains of **6** into a 3D supramolecular network. (For interpretation of the references to colour in this figure legend, the reader is referred to the web version of this article.)

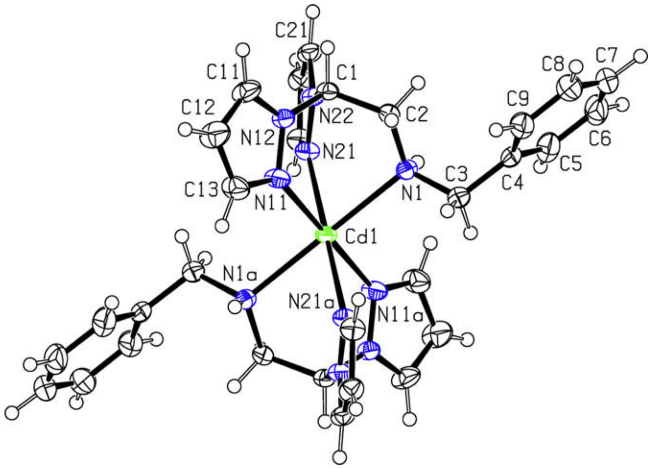

Fig. 10. ORTEP diagram of cationic $\{Cd[(pz)_2CHCH_2NHCH_2C_6H_5]_2\}^{2+}$ building block of **7**.

brown solid (12.0 g, 60.5%). HRMS (direct probe): calcd. for $C_8H_{11}N_5$ 178.1093, found 178.1088. ^1H NMR (300 MHz, $CDCl_3$) δ_H 7.60, 7.58 (d, d; *J* = 1, 2 Hz; 2H, 2H; H_3,H_5-pz), 6.37 (t, *J* = 7 Hz, 1H, CH), 6.30 (d, d, *J* = 2, 1 Hz, 2H, H_4-pz), 3.78 (d, *J* = 7 Hz, 2H, CH_2), 1.68 (br s, 2H, NH_2).

4.3. Synthesis of $C_6H_5CH_2NHCH_2CH(pz)_2$ (**2**)

Compound **1** (3.54 g, 0.020 mol) was dissolved in methanol (75 mL). Once completely dissolved, benzaldehyde (2.0 mL, 0.020 mol) was added and the mixture was heated at reflux overnight. After cooling to room temperature, excess of $NaBH_4$ (1.50 g, 0.040 mol) was added in portions and the mixture stirred for 6 h. The solvent was removed via rotary evaporation and the residue was dissolved in ethyl acetate (75 mL). The organic layer was washed with three 100 mL aliquots of water, dried over anhydrous sodium sulfate, filtered, and then the solvent removed via rotary evaporation to yield the product as a sticky yellow solid (4.92 g, 92%). HRMS (direct probe): calcd. for $C_{15}H_{17}N_5$: 267.1484, found 267.1483. ^1H NMR (300 MHz, $CDCl_3$) δ_H 7.58, 7.56 (d, d; *J* = 1, 2 Hz; 2H, 2H; H_3,H_5-pz), 7.25 (m, 5H, C_6H_5), 6.52 (t, *J* = 7 Hz, 1H, CH), 6.28 (dd, *J* = 2, 1 Hz, 2H, H_4-pz), 3.82 (s, 2H, C_6H_5–CH_2) 3.69 (d, *J* = 7 Hz, 2H, N–CH_2).

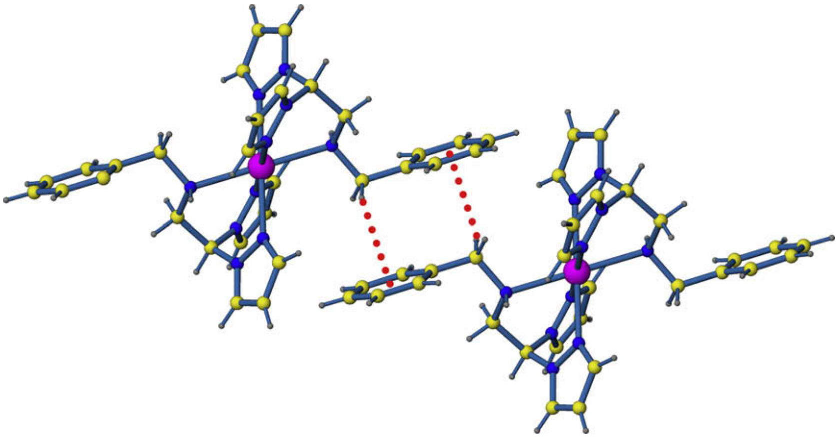

Fig. 11. 1D supramolecular organization of **7** into chains via C–H···π interactions between backbone hydrogens and benzyl rings (dotted red lines). (For interpretation of the references to colour in this figure legend, the reader is referred to the web version of this article.)

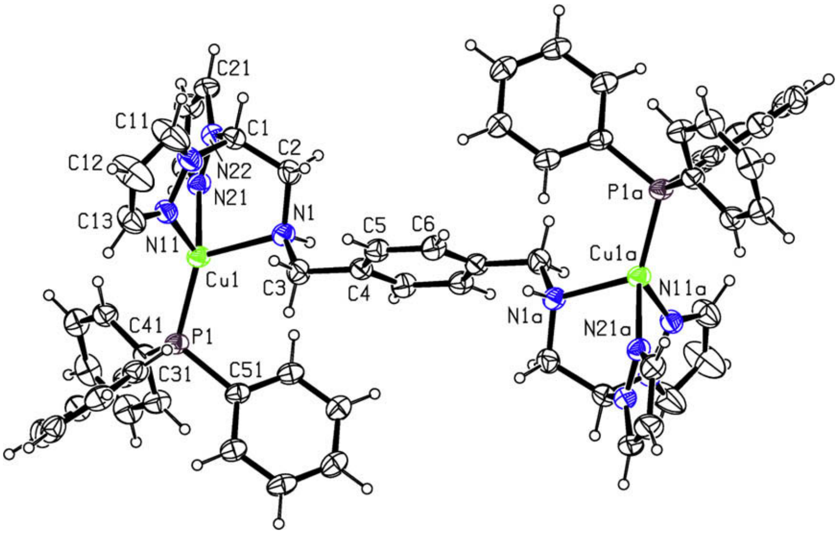

Fig. 12. ORTEP diagram of cationic $\{[(PPh_3)Cu]_2[p\text{-}((pz)_2CHCH_2NHCH_2)_2C_6H_4]\}^{2+}$ building block of **8**. Displacement ellipsoids drawn at the 30% probability level.

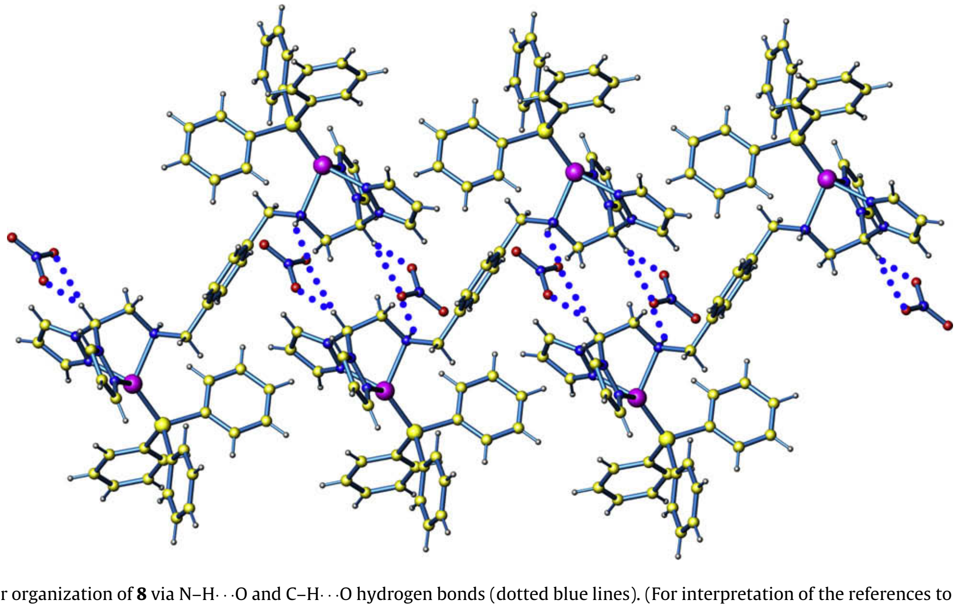

Fig. 13. 1D supramolecular organization of **8** via N–H···O and C–H···O hydrogen bonds (dotted blue lines). (For interpretation of the references to colour in this figure legend, the reader is referred to the web version of this article.)

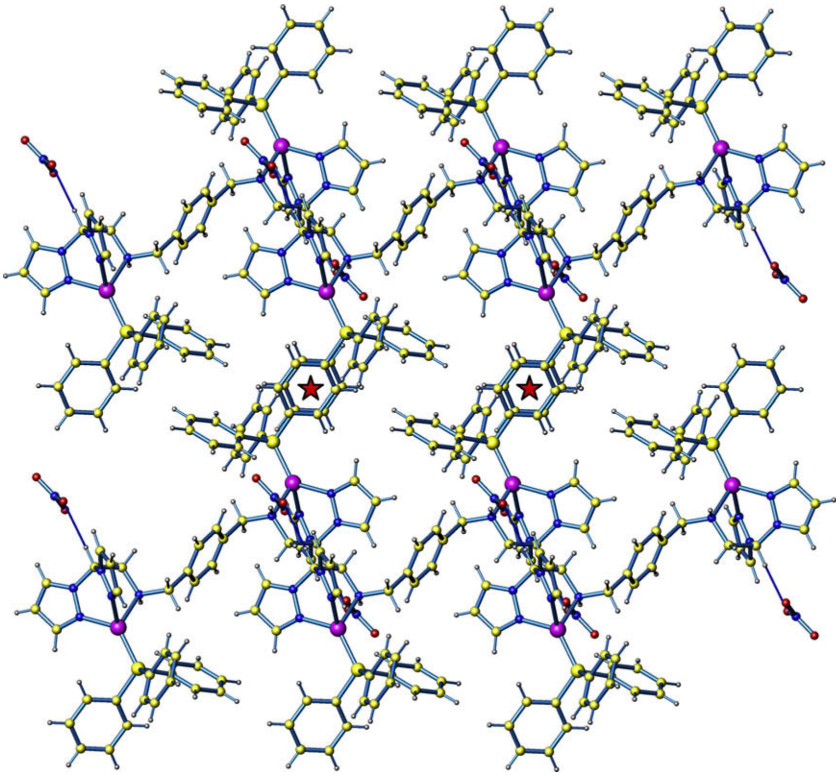

Fig. 14. 2D supramolecular organization of **8**. Red stars show π–π stacking sites. (For interpretation of the references to colour in this figure legend, the reader is referred to the web version of this article.)

4.4. Synthesis of *p*-$C_6H_4(CH_2NHCH_2CH(pz)_2)_2$ (**3**)

Compound **3** was synthesized by two different methods. In the first synthesis, **1** (1.76 g, 9.93 mmol) was dissolved in THF (100 mL), placed under a nitrogen atmosphere and triethylamine (0.50 g, 4.9 mmol) added via syringe. Dibromo-*para*-xylene (1.30 g, 4.92 mmol) was dissolved in THF (50 mL) and slowly added via syringe. The solution was stirred for 1 h, then heated at reflux overnight. After cooling, the solution was filtered, the solvent removed via rotary evaporation, the resulting yellow oil extracted with water and ethyl acetate, the organic layer dried over anhydrous sodium sulfate, filtered, and the solvent removed by rotary evaporation to yield 0.75 g of product. As this product was impure, it was dissolved in boiling ethanol and chilled overnight. The pure product formed as 0.21 g of a beige powder (0.46 mmol, 15.9%). In the second synthesis, compound **1** (3.54 g, 0.020 mol) was dissolved in ethanol (100 mL) with terephthalaldehyde (1.34 g, 0.010 mol) and heated at reflux overnight. After cooling with an ice bath, $NaBH_4$ (1.13 g, 0.030 mol) was added in small portions and the solution was heated at reflux for 72 h. The solution was filtered, the solvent was removed via rotary evaporation, the residue redissolved in chloroform (75 mL), filtered, and dried. This chloroform-soluble fraction was dissolved in hot methanol (50 mL), filtered, and dried to give **3** as a light yellow powder of high purity (0.32 g, 38%). HRMS (direct probe): calcd. for $C_{24}H_{28}N_{10}$ 457.2576, found 457.2578. *Anal.* Calc. for $C_{24}H_{28}N_{10}$: C, 63.14; H, 6.18; N, 30.68. Found: C, 63.35; H, 5.85; N, 30.33%. ^1H NMR (300 MHz, $CDCl_3$) δ_H 7.60, 7.58 (d, d; *J* = 1, 2 Hz; 4H, 4H; H_3,H_5-pz), 7.20 (s, 4H, C_6H_4), 6.55 (t, *J* = 7 Hz, 2H, CH), 6.25 (dd, *J* = 1, 2 Hz, 4H, H_4-pz), 3.80 (d, *J* = 7 Hz, 4H, N–CH_2), 3.67 (br s, 4H, C_6H_4–CH_2), 2.18 (br s, 2H, NH).

4.5. Synthesis of $\{(PPh_3)Cu[(pz)_2CHCH_2NH_2]\}NO_3$ (**4**)

Compound **1** (0.029 g, 0.16 mmol) and $[Cu(PPh_3)_2]NO_3$ (0.108 g, 0.16 mmol) were dissolved in dichloromethane (20 mL). The solution was stirred for 15 min and hexanes (100 mL) were added yielding a pale yellow powder (0.127 g, 95%). *Anal.* Calc. for $C_{26}H_{26}CuN_6O_3P$: C, 55.27; H, 4.64; N, 14.87. Found: C, 54.97; H, 4.61; N, 15.11%. Layering a dichloromethane solution of the product with hexanes yielded single crystals suitable for X-ray diffraction studies.

4.6. Synthesis of $\{(PPh_3)Cu[(pz)_2CHCH_2NHCH_2C_6H_5]\}NO_3$ (**5**)

Compound **2** (0.044 g (0.16 mmol) and $[Cu(PPh_3)_2]NO_3$ (0.108 g, 0.16 mmol) were dissolved in dichloromethane (20 mL). The solution was stirred for 15 min and hexanes (100 mL) were added yielding a pale yellow powder (0.123 g, 89%). *Anal.* Calc. for $C_{33}H_{32}CuN_6O_3P$: C, 60.50; H, 4.92; N, 12.83. Found: C, 60.72; H, 5.32; N, 12.41%. Layering a dichloromethane solution of the product with hexanes yielded single crystals suitable for X-ray diffraction studies.

4.7. Synthesis of $\{(N_3)_2Cu[(pz)_2CHCH_2NHCH_2C_6H_5]\}$ (**6**)

Compound **2** (0.028 g, 0.10 mmol) was dissolved in dichloromethane (20 mL). Copper(II) acetate monohydrate (0.020 g, 0.10 mmol) and sodium azide (0.010 g, 0.10 mmol) were dissolved in methanol (20 mL). The two solutions were layered in a test tube and a small quantity of X-ray quality crystals were obtained in several days.

4.8. Synthesis of $\{Cd[(pz)_2CHCH_2NHCH_2C_6H_5]_2\}(PF_6)_2\cdot 3C_3H_6O$ (**7**)

To a methanolic solution of $(pz)_2CHCH_2NHCH_2C_6H_5$ (0.267 g, 1.00 mmol) was added dropwise concentrated HCl until pH 2. The solvents were removed by rotary evaporation and the residue was redissolved in water (50 mL). To this solution an excess of a saturated aqueous solution of NH_4PF_6 (ca. 1.0 g in 75 mL water) was added dropwise, resulting in the precipitation of

[$(pz)_2CHCH_2NH_2CH_2C_6H_5$]$PF_6$ (0.37 g, 89%). [$(pz)_2CHCH_2NH_2CH_2$-C_6H_5]PF_6 (0.103 g (25 mmol) was dissolved in acetone and added to a solution of $Cd(acac)_2$ (0.038 g, 12.5 mmol) in acetone under stirring yielding {Cd[$(pz)_2CHCH_2NHCH_2C_6H_5$]$_2$}$(PF_6)_2$ (0.100 g, 86 %) as an off-white powder. A portion of this solid was then dissolved in acetone in a small vial, sealed in a larger tube containing diethyl ether, and X-ray quality crystals of (**7**) formed after several days.

*4.9. Synthesis of {[$(PPh_3)Cu$]$_2$[p-($(pz)_2CHCH_2NHCH_2)_2C_6H_4$]}$(NO_3)_2$·solvate (**8**)*

$Cu(PPh_3)_2NO_3$ (0.130 g, 0.32 mmol) and half an equivalent of **3** (0.045 g, 0.16 mmol) were each dissolved in dichloromethane (10 mL). The two solutions were combined and stirred. The resulting solution was layered with hexanes in capped vials, from which X-ray quality crystals were obtained overnight. HRMS ESI(+) *m*/*z*: calcd. for [$(C_{60}H_{58}Cu_2N_{10}P_2)NO_3$]$^+$ 1168.2792, found 1168.2762.

4.10. Crystallographic studies

Crystal information, data collection, and refinement parameters are given in Tables 1 and 2. For all five complexes X-ray intensity data were measured at 150(1) K on a Bruker SMART APEX CCD-based diffractometer system (Mo Kα radiation, $\lambda = 0.71073$ Å) [7]. Raw data frame integration and Lorentz-polarization corrections were performed with SAINT+ [7]. Direct methods structure solution, difference Fourier calculations, and full-matrix least-squares refinement against F^2 were performed with SHELXTL [8].

For compound **4**, final unit cell parameters were determined by least-squares refinement of 7990 reflections from the data set with $I > 5\sigma(I)$. No absorption correction was applied. The compound crystallizes in the space group $P2_1/c$. There is one complete formula unit in the asymmetric unit. Non-hydrogen atoms were refined with anisotropic displacement parameters; hydrogen atoms were placed in idealized positions and included as riding atoms.

For compound **5**·$1.5CH_2Cl_2$, final unit cell parameters were determined by least-squares refinement of 7074 reflections with $I > 5\sigma(I)$ from the data set. The data were corrected for absorption effects with SADABS [7]. The compound crystallizes in the triclinic system. The space group $P\bar{1}$ was confirmed by the successful solution and refinement of the data. The asymmetric unit contains a {$(PPh_3)Cu$[$(pz)_2CHCH_2NHCH_2C_6H_5$]}NO_3 cation-anion pair, and 1.5 independent CH_2Cl_2 molecules of crystallization. The CH_2Cl_2 molecules are disordered. C61/Cl1/Cl2 is disordered about a general position; C71–Cl6 is disordered about an inversion center and was modeled as two independent partial molecules with occupancies fixed at 0.35 and 0.15. A total of 31 restraints were used to maintain chemically reasonable geometries for these species. Eventually all non-hydrogen atoms were refined with anisotropic displacement parameters except those disordered atoms with occupancies <0.5. Hydrogen atoms were placed in geometrically idealized positions and included as riding atoms with the exception of the nitrogen-bound H1A, which was located and refined freely.

For compound **6**, final unit cell parameters were determined by least-squares refinement of 7008 reflections with $I > 5\sigma(I)$ from the data set. The compound crystallizes in the triclinic system. The space group $P\bar{1}$ was assumed and confirmed by the successful solution and refinement of the data. The asymmetric unit consists of two crystallographically independent molecules. All non-hydrogen atoms were refined with anisotropic displacement parameters. Hydrogen atoms bonded to carbon were placed in geometrically idealized positions and included as riding atoms with refined isotropic displacement parameters. The nitrogen-bound hydrogens H1N and H2N were refined isotropically subject to an N–H = 0.84(2) Å distance restraint.

For compound **7**, final unit cell parameters were determined by least-squares refinement of 5645 reflections with $I > 5\sigma(I)$ from the data set. The compound crystallizes in the triclinic crystal system. The space group $P\bar{1}$ was confirmed by the successful solution and refinement of the data. The asymmetric unit consists of half of the {Cd[$(pz)_2CHCH_2NHCH_2C_6H_5$]$_2$}$^{2+}$ complex located on an inversion center, one PF_6^- anion, and 1.5 independent acetone molecules of crystallization. The half-acetone is disordered about an inversion center. The ligand is disordered over two closely spaced orientations in the refined ratio $A/B = 0.701(4)/0.299(4)$. The disorder affects only the -$CH_2NHCH_2C_6H_5$ part of the ligand; the $CH(pz)_2$ part is normal. The total population of the two disorder components was constrained to sum to unity. The geometry of the minor component was restrained to be similar to that of the major with a SHELX SAME instruction (21 restraints). Counterpart atoms in each component were refined with common displacement parameters (e.g., $U_{ij}(N1A) = U_{ij}(N1B)$, etc.). All non-hydrogen atoms were refined with anisotropic displacement parameters. Hydrogen atoms were placed in geometrically idealized positions and included as riding atoms, with the exception of the nitrogen proton H1NA of the major disorder component, which was located and refined freely.

For compound **8**, final unit cell parameters were determined by least-squares refinement of 6455 reflections with $I > 5\sigma(I)$ from the data set. The compound crystallizes in the triclinic system. The space group $P\bar{1}$ was confirmed by the successful solution and refinement of the data. The asymmetric unit contains half a {[$(PPh_3)Cu$]$_2$[*p*-($(pz)_2CHCH_2NHCH_2)_2C_6H_4$]}$^{2+}$ complex located on an inversion center, one NO_3^- anion and a region of severely disordered solvent centered at (½, 0, ½). The disordered solvent could not be modeled reasonably and was therefore accounted for with the SQUEEZE program in PLATON [9]. The solvent occupies a volume of 448.0 Å^3 per unit cell, corresponding to 148 e$^-$/cell. The contribution of these species was removed from subsequent structure factor calculations. Note that the reported FW, d_{calc} and *F* (0 0 0) refer to known unit cell contents only. Based on unsuccessful disorder models, the included solvent is most likely CH_2Cl_2. All non-hydrogen atoms were refined with anisotropic displacement parameters. Hydrogen atoms were placed in geometrically idealized positions and included as riding atoms except for H1N, which was located and refined freely.

Acknowledgment

The authors thank the National Science Foundation (CHE-0715559) for support.

Appendix A. Supplementary material

CCDC 613951, 613952; 706338, 706339, 706340 contain the supplementary crystallographic data for this paper. These data can be obtained free of charge from The Cambridge Crystallographic Data Centre via www.ccdc.cam.ac.uk/data_request/cif. Supplementary data associated with this article can be found, in the online version, at doi:10.1016/j.ica.2009.06.004.

References

[1] (a) D. Braga, L. Brammer, N.R. Champness, Cryst. Eng. Commun. 7 (2005) 1;
(b) L. Brammer, Chem. Soc. Rev. 33 (2004) 476;
(c) S. James, Chem. Soc. Rev. 32 (2003) 276;
(d) C. Janiak, J. Chem. Soc., Dalton Trans. (2003) 2781;
(e) C.V.K. Sharma, Cryst. Growth Des. 2 (2002) 465.
[2] (a) D.L. Reger, J.D. Elgin, R.F. Semeniuc, P.J. Pellechia, M.D. Smith, Chem. Commun. (2005) 4068;
(b) D.L. Reger, R.F. Semeniuc, V. Rassolov, M.D. Smith, Inorg. Chem. 43 (2004) 537;
(c) D.L. Reger, R.F. Semeniuc, M.D. Smith, Inorg. Chem. 42 (2003) 8137;

(d) D.L. Reger, R.F. Semeniuc, V. Rassolov, M.D. Smith, J. Organomet. Chem. 666 (2003) 87;
(e) D.L. Reger, J.R. Gardinier, R.F. Semeniuc, M.D. Smith, J. Chem. Soc., Dalton Trans. (2003) 1712;
(f) D.L. Reger, T.D. Right, R.F. Semeniuc, T.C. Grattan, M.D. Smith, Inorg. Chem. 40 (2001) 6212;
(g) D.L. Reger, R.F. Semeniuc, M.D. Smith, Inorg. Chem. 40 (2001) 6545.
[3] S. Trofimenko, J. Am. Chem. Soc. 92 (1970) 5118.
[4] (a) S. Trofimenko, Scorpionates: The Coordination Chemistry of Polypyrazolylborate Ligands, Imperial College Press, London, 1999;
(b) C. Pettinari, Scorpionates II: Chelating Borate Ligands, Imperial College Press, London, 2008.
[5] (a) D.L. Reger, E.A. Foley, R.F. Semeniuc, M.D. Smith, Inorg. Chem. 46 (2007) 11345;
(b) D.L. Reger, R.P. Watson, M.D. Smith, Inorg. Chem. 45 (2006) 10077;
(c) D.L. Reger, R.P. Watson, J.R. Gardinier, M.D. Smith, Inorg. Chem. 43 (2004) 6609.
[6] D.L. Reger, R.F. Semeniuc, J.R. Gardinier, J. O'Neal, B. Reinecke, M.D. Smith, Inorg. Chem. 45 (2006) 4337.
[7] SMART Version 5.625, SAINT+ Version 6.22 and SADABS Version 2.05, Bruker Analytical X-ray Systems, Inc., Madison, Wisconsin, USA, 2001.
[8] G.M. Sheldrick, SHELXTL Version 6.1, Bruker Analytical X-ray Systems, Inc., Madison, Wisconsin, USA, 2000.
[9] (a) A.L. Spek, Acta Crystallogr., Sect. A 46 (1990) 194;
(b) A.L. Spek, PLATON: A Multipurpose Crystallographic Tool, Utrecht University, Utrecht, The Netherlands, 1998.